INFLUENCE OF OPTICAL BAND STRUCTURES ON THE DIFFRACTION OF PHOTONIC COLLOIDAL CRYSTALS

WILLEM L. VOS[1], RUDOLF SPRIK[1], AD LAGENDIJK[1,2], GERARD H. WEGDAM[1], ALFONS VAN BLAADEREN[2,3] AND ARNOUT IMHOF[3]

[1] *van der Waals-Zeeman Instituut, Universiteit van Amsterdam, 1018 XE Amsterdam, The Netherlands*

[2] *FOM Institute for Atomic and Molecular Physics 1098 SJ Amsterdam, The Netherlands*

[3] *van 't Hoff Laboratorium, Universiteit van Utrecht, 3584 CH Utrecht, The Netherlands*

Abstract. We have performed optical diffraction studies on colloidal crystals with large refractive index mismatches up to 1.45 and polarizibilities per volume as large as 0.6. These conditions push colloidal crystals into the regime where strong coupling between photonic crystals and the light field occurs. It is found that the photonic band structures result in apparent Bragg spacings that strongly depend on the wavelength of light. The dynamical diffraction theory that correctly describes weak photonic effects encountered in X-ray diffraction, also breaks down. Two simple models are presented that give a much better description of the diffraction of photonic crystals.

1. Introduction

Photonic crystals are 3-dimensional (3D) periodic composites of different dielectric materials, with lattice parameters of the order of the wavelength of light[1]-[7]. Light that travels through such structures experiences a periodic variation of the refractive index, analogous to the periodic potential energy of an electron in an atomic crystal. Therefore, the dispersion curves of light become organized in bands in a Brillouin zone in reciprocal space called photonic band structures. Variation of the refractive index causes a splitting of the bands at the edges of the Brillouin zone, that are called stop gaps. No waves can propagate for energies within these gaps. The same principle underlies the functioning of dielectric mirrors [8], which can thus be regarded as 1D photonic crystals. The stop gaps widen with increasing modulation of the refractive index. Ultimately, the stopgaps in all directions will overlap and give rise to a complete photonic band gap [1, 2] for refractive index ratios larger than 1.9, a polarizibility α per 'atomic' volume v (times 4π) larger than 0.5, and suitable crystal structures - e.g. the diamond structure [9]. In this case, no wave with an energy within the gap can propagate through the crystal in *any* direction; the crystal acts as a 3D mirror. A fascinating situation arises when an excited atom or molecule with an excitation energy within the band gap is placed inside a photonic crystal. Spontaneous emission is no longer possible, and the atom is trapped in its excited state. This is a spectacular phenomenon in quantum electrodynamics,

where it was believed for a long time that spontaneous emission is an intrinsic property of an atom [10]. Although this situation has not yet been observed experimentally, exciting prospects such as threshholdless lasers and diodes have already been discussed [10]. In another analogy with electronics, John [2] has predicted that some disorder in the crystal will result in localized states inside the band gap, similar to excitons in a semiconductor band gap.

The term photonic band gap was introduced by Yablonovitch [1] but experimental observations have only been made in the microwave regime down to wavelengths of about $\lambda \sim 500$ μm [6]. It is clearly a tremendous challenge to scale the fabrication techniques of photonic structures down to reach the optical part of the spectrum ($400 < \lambda < 800$ nm). The group of Scherer (Caltech) has managed to drill holes of several hundred nm in slabs of GaAs [7]. A disadvantage of this method, however, is that crystals of only a few unit cells thickness can be made, which is insufficient for the creation of a complete optical band gap. In addition, this fabrication technique is very difficult.

A different approach is to make photonic crystals with colloidal suspensions [11]. These are, e.g., solid particles with radii r between roughly 1 and 1000 nm that are suspended in liquids or gases [12]. It is possible to synthesize particles with dimensions uniform to within a few percent, which can spontaneously nucleate crystals at sufficiently high density or low enough salt concentration [13]. If the lattice parameter a is of the order of optical wavelengths, crystal reflections can be visually observed as a beautiful iridescence [14]. Optical diffraction has been applied to identify various crystal structures in systems with low refractive index contrasts or low densities ($4\pi\alpha/v < 0.05$) [13], [15]-[17]. Optical photonic experiments have already been done on similar weakly photonic crystals by Asher *et al* [18], Martorell and Lawandy [19], and Herbert and Malcuit [20]. These demonstrate the use of colloidal crystals to applications in photonics.

In this paper, we present a study of colloidal crystals with refractive index ratios up to 1.45 and 'photonic strengths' ($4\pi\alpha/v < 0.05$) up to 0.6. The experiments are a significant advance towards the use of these systems in the strongly photonic regime. Diffraction experiments have been done to investigate both the optical band structures and the crystal structure. With increasing photonic strength, the band structures result in apparent Bragg spacings that strongly depend on the wavelength. Even the dynamical diffraction theory [21, 22], that is well-known in X-ray diffraction (where $4\pi\alpha/v \sim 10^{-4}$) fails to describe the observations. We present two simple models that give physically more reliable results for the lattice spacings of strongly scattering photonic crystals: firstly by combining Bragg's law with linear bands using an averaged refractive index, and secondly using periodically stratified dielectric media [8]. Earlier accounts of this work have appeared in Ref. [23, 24].

2. Theory

In a diffraction experiment, one observes crystal reflections if the incoming and outgoing wave vectors $\mathbf{k}_{\rm in}$ and $\mathbf{k}_{\rm out}$ yield a difference vector equal to a reciprocal lattice vector $\mathbf{G}_{\rm hkl}$: $\mathbf{k}_{\rm out} - \mathbf{k}_{\rm in} = \mathbf{G}_{\rm hkl}$, with hkl the Miller indices [25]. The length of the wave vector inside the crystal is $|\mathbf{k}| = (2\pi n)/\lambda$, with n the refractive index of the crystal, λ the wavelength of light in vacuum. The length of $\mathbf{G}_{\rm hkl}$ is: $|\mathbf{G}_{\rm hkl}| = 2\pi/d_{\rm hkl}$, with d_{hkl} the lattice spacing of the hkl crystal planes. For weak photonic strengths, the dispersion relation between the energy E and the wave vectors is linear: $E = c|\mathbf{k}|$, and we obtain the well-known Bragg law: $d_{\rm Bragg} = \lambda/(2n_{\rm med} sin\theta)$. Here, 2θ is the diffraction angle subtended between the incoming and outgoing wave vectors $\mathbf{k}_{\rm in}$ and $\mathbf{k}_{\rm out}$, $n_{\rm med}$ is the refractive index of the medium in which the particles are suspended (see Fig. 1). With increasing photonic strengths, the dispersion curves become non-linear, and stopgaps appear at the edges of the Brillouin zone. The diffraction condition is modified compared to the Bragg case and fulfilled at a lower energy (Fig. 1).

In the limit of weak photonic strengths, improvements on the Bragg law can be calculated exactly with the dynamical diffraction theory [21, 22], that is well known for X-ray diffraction ($4\pi\alpha/v \sim 10^{-4}$). The relation between the lattice spacing $d_{\rm dyn}$ and the diffraction angle is for specular reflections:

$$d_{\rm dyn} = \frac{\lambda}{2n_{\rm med}sin\theta}\left(1+\frac{\Psi}{2sin^2\theta}\right)^{-1} , \tag{1}$$

with

$$\Psi = 3\phi\frac{m^2-1}{m^2+2} , \tag{2}$$

where ϕ is the volume fraction of colloidal spheres, m is the ratio of the refractive index of the spheres and the medium: $m = n_{\rm sph}/n_{\rm med}$, and Ψ is a photonic strength parameter that measures the interaction strength of the light and photonic crystal. Equation 1 can be heuristically derived - albeit with a different Ψ parameter - by considering Bragg diffraction as an interference between two light rays that are reflected from two crystalline layers (such as depicted in most elementary texts, e.g. [25]) and correcting for the extra optical path length that the second light ray experiences while twice traversing the upper layer. The parameter Ψ can be rewritten as:

$$\Psi = 4\pi\frac{\alpha}{v} . \tag{3}$$

Now it becomes clearer that Ψ is a good choice for a photonic strength parameter, because it can be physically interpreted as the ratio between the "optical" volume and the actual volume of the scattering particles. The effects of photonic strength become more apparent for smaller θ or larger $d_{\rm hkl}/\lambda$, which corresponds to higher bands in Fig. 1. Therefore, it is very useful to do a diffraction experiment as a function of wavelength on a photonic crystal: in the short wavelength limit one will mostly probe the effects of photonic band structures (through $\mathbf{k}_{\rm in}$ and $\mathbf{k}_{\rm out}$), whereas in the long wavelength limit will mostly characterize the reciprocal lattice vectors and hence the crystal structure. Finally, we observe that an increase of Ψ for a given crystal structure and constant lattice parameter results in an increase of the diffraction angle 2θ.

3. Experimental

Crystals were grown from silica spheres ($n_{\rm sph} = 1.45$) with radii between 108 and 525 nm, suspended in dimethylformamide (DMF), ethanol, and water ($n_{\rm med} = 1.43,\ 1.36,\ 1.33$ respectively). For details of the synthesis and characterization of the spheres, see Refs. [26]-[28]. The samples crystallized after sedimentation under gravity in 400 μm thick and 4 mm wide glass capillaries (Vitro Dynamics). In addition, one charge stabilized system was studied, that started to crystallize immediately after loading and sealing capillaries. Crystals in air ($n_{\rm med} = 1.00$) were made from sedimented crystals by letting the suspending liquid evaporate slowly in several weeks.

The capillaries were mounted in a cilindrical bath containing glycerine ($n = 1.47$), that closely matches the refractive index of the capillaries. This bath was mounted on a stage that could be fully rotated (ω-circle), see Fig. 2. Because colloidal crystals often order with the close packed planes parallel to the walls of the cell (see e.g. [29, 30]), upon rotating the samples, the diffracted intensity of these crystal planes becomes very strong and clearly visible on a screen if it coincides with the specularly reflected laser beam. Incident monochromatic light with wavelengths λ between 458 and 785 nm was collimated, modulated, and polarized. Scattered radiation was collimated, polarization analyzed, and detected with a photo diode, all of which were mounted on an independently rotating stage (2θ-circle). In all experiments V-V polarization was used. The measured values of 2θ were corrected for refraction at the

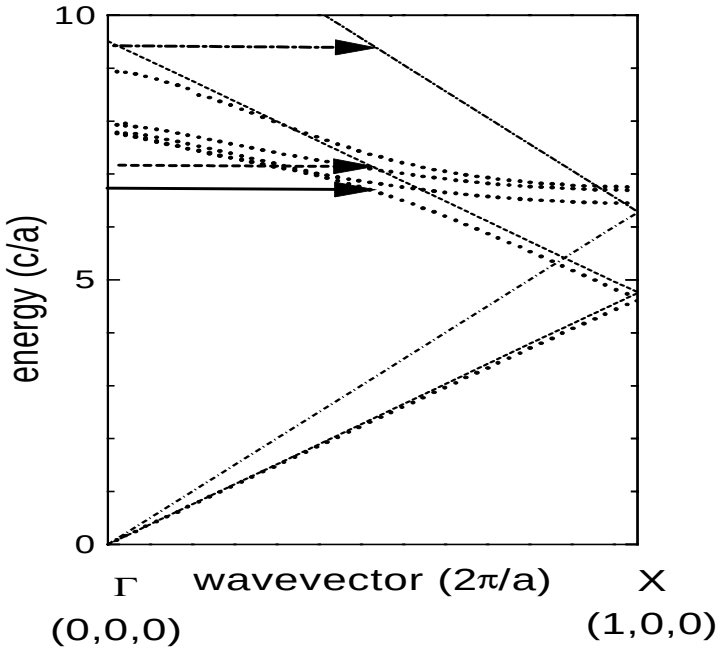

Figure 1. Bandstructures calculated with the plane-wave method [3, 4, 5] for the 100 (X) direction of an f.c.c. crystal with 74 vol% spheres (dots). For a complementary theoretical method, see Ref. [35]. Spheres with index $n_{\rm sph} = 1.45$ and medium with $n_{\rm med} = 1.0$ were taken, corresponding to $\Psi = 0.6$. At $E = 6.7$, the first folding of the Brillouin zone occurs. [25]. For clarity, only lower bands have been plotted. The incoming wavevectors $\mathbf{k}_{\rm in}//\mathbf{100}$ taking part in the diffraction by a reciprocal lattice vector $\mathbf{G}_{\rm hkl}$ with $hkl = 111$ have been indicated. The drawn arrow at $E = 6.7$ is $\mathbf{k}_{\rm in}$ corresponding to the full photonic bandstructure. The dashed arrow at $E = 7.2$ is $\mathbf{k}_{\rm in}$ corresponding to the linear bands with a slope that is inversely proportional to the average refractive index $n_{\rm cryst}$ at $|\mathbf{k}| = \mathbf{0}$ (dashed lines). The dashed-dotted arrow at $E = 9.4$ is $\mathbf{k}_{\rm in}$ corresponding to the Bragg law: linear bands with a slope that is inversely proportional to the refractive index of the medium $n_{\rm med}$ (dashed-dotted lines).

bath-capillary-crystal interfaces and offset errors were eliminated by scanning both positive and negative 2θ angles.

4. Results

Representative diffraction patterns of close packed lattice planes at $\lambda = 633$ nm for samples with increasing photonic parameters, but comparable lattice parameters are shown in Fig. 3. Crystals with $\Psi = 0.017$ reveal sharp diffraction lines near $2\theta = 75^o$ which corresponds to a lattice spacing $d_{\rm hkl} = 380$ nm. For $\Psi = 0.115$, the diffraction peak is shifted to a larger scattering angle of 80^o. This is caused by an increase of Ψ and also by a decrease of the total refractive index of the system, whereas $d_{\rm hkl} = 370$ nm. For $\Psi = 0.60$, the diffraction angle has moved to 97^o. This is caused by the increase of Ψ, in addition by the decrease of the total refractive index of the system, and a slightly smaller $d_{hkl} = 350$ nm. The diffracted signal appears to consist of several fringe-like features. Whereas we understand the position of the band as a whole, we have no explanation for the fringes but can exclude several possibilities; These are not caused by interference in the walls of the capillary (300 μm thick), which would give a fringe period of 0.04^o. Also, at the index contrast involved ($m = 1.45$), the Mie scattering of the spheres does not produce sharp and closely spaced resonances. Moreover,

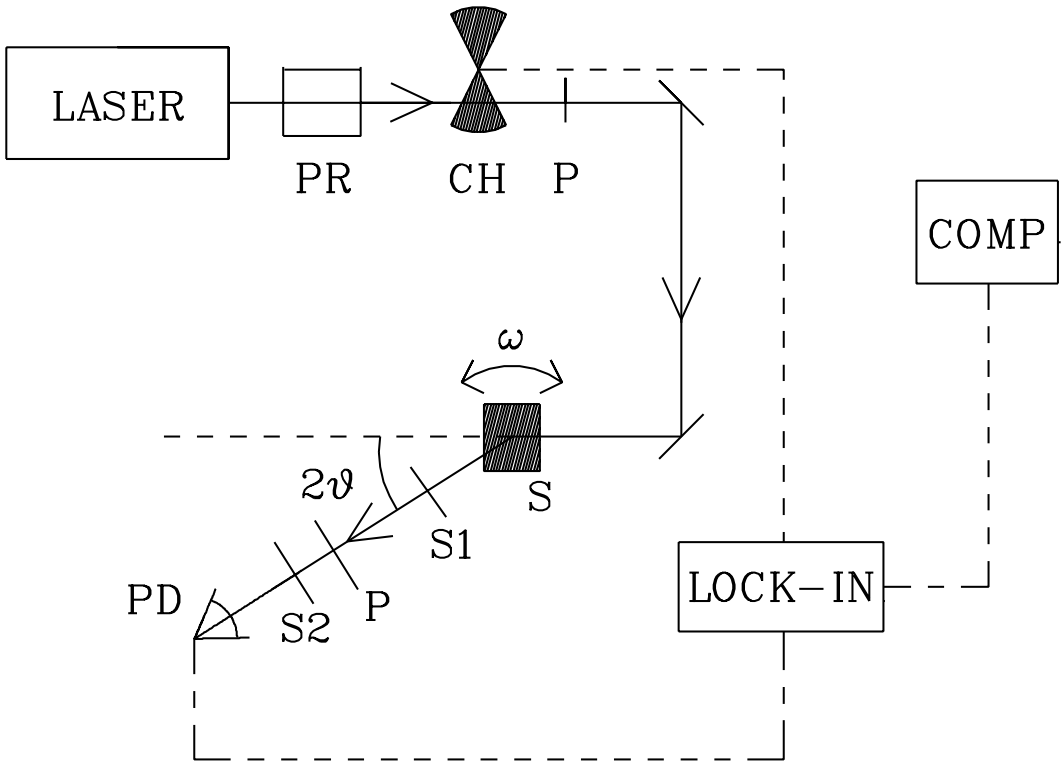

Figure 2. Schematic drawing of the light scattering setup. Light emanates from a laser, is polarization rotated (PR), modulated by a chopper (CH), and polarized (P). It is scattered in the sample (S) that is mounted in an index matching bath (not shown) that sits on a rotation table (ω-circle). Scattered light at an independent angle 2θ is collimated through slits S1 and S2, polarization analyzed (P), and collected with a photo diode (PD). The signal from the diode is discriminated with a lock-in amplifier and stored in a computer (comp).

reducing Ψ of such a sample to 0.017 by reintroducing liquid DMF in the capillary results again in a single sharp diffraction peak near $2\theta = 75^o$, identical to the lower diffraction pattern in Fig. 3. Therefore, it is concluded that samples with increasing Ψ produce diffraction peaks at higher diffraction angle, which is so far consistent with the dynamical theory. We note that the volume fractions of the spheres in the crystals that are calculated from the lattice spacings and the known radii of the spheres, agree with estimates obtained from the volume fraction of the starting suspension and the ratio of the volumes of the crystal formed and the total sample.

From the measured diffraction angle 2θ, the Bragg spacing d_{Bragg} and the dynamic spacing d_{dyn} between the close packed lattice planes are calculated and plotted in Fig. 4. For Ψ=0.017, Fig. 4a reveals that d_{Bragg} decreases slightly as a function of wavelength. The values of d_{dyn} are lower and nearly independent of wavelength, the difference with d_{Bragg} decreasing to long wavelengths as expected. A similar result was obtained for a dilute charged system with $\Psi = 0.005$. In contrast, the results for $\Psi = 0.115$ show a strong increase of d_{Bragg} of 50% in going from 785 to 458 nm (Fig. 4b). This means that d_{Bragg} has become an unphysical estimate of the lattice spacing. A more reliable result is obtained with the dynamic theory, because d_{dyn} is independent of wavelength. At the longest wavelengths, d_{Bragg} converges to d_{dyn} as expected from Eq. (1). This confirms that long wavelength extrapolations may be used to estimate the real lattice spacings of photonic crystals. Similar results were obtained for a sample with $\Psi = 0.067$. For $\Psi = 0.60$, Fig. 4c reveals a giant increase of d_{Bragg} with decreasing wavelength. For this strongly scattering sample, it appears that the dynamic theory is also not appropriate anymore, because d_{dyn} clearly decreases with decreasing wavelength. Furthermore, the values

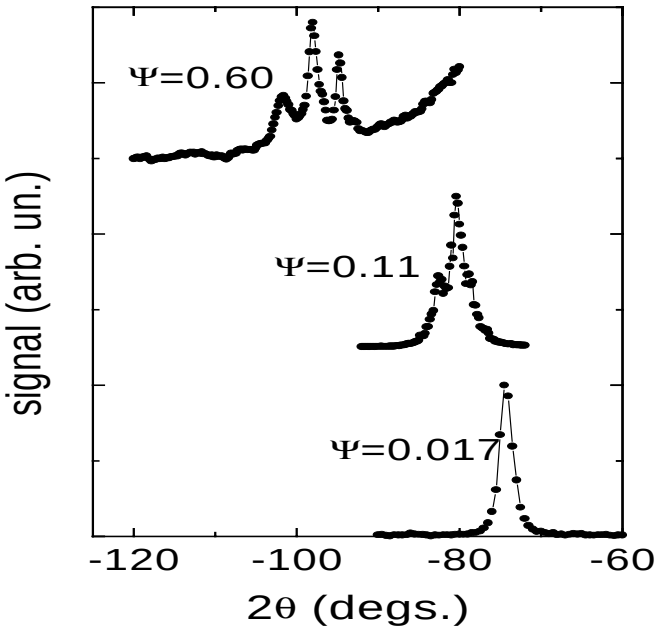

Figure 3. Diffraction patterns of colloidal crystals. The diffraction patterns have been normalized and offset for clarity. From bottom to top: spheres with $r = 211$ nm in DMF ($\Psi = 0.017$), in water ($\Psi = 0.11$), and in air ($\Psi = 0.6$).

of $d_{\rm dyn}$ would imply that the colloidal spheres are strongly overlapping. With increasing wavelength, both apparent lattice spacings converge to a value expected for touching close packed spheres (344 nm). We can exclude the possibility that the dispersive effects are caused by a smearing of the reciprocal lattice points due to mixed hexagonal stacking, because smearing does not happen for close packed lattice planes [13, 31].

5. Discussion

We have used two simple models that go beyond dynamical diffraction theory to describe the relation between the diffraction angle, the wavelength, and the crystal structure and lattice parameter. The first model consists of approximating the apparent spacings $d_{\rm Bragg}$ and $d_{\rm dyn}$ of every *hkl* reflection with the apparent spacings of pairs of layers of dielectric materials. This is similar to the conventional approach to stratified dielectric systems such as dielectric mirrors [8]. One layer of each pair is assigned the refractive index $n_{\rm sph}$ of the colloidal spheres and the other that of the medium ($n_{\rm med}$). The thickness d of each pair of layers is fixed to the expected lattice spacing d_{hkl}. The relative thickness of the layers is determined by the volume fraction of spheres ϕ, which is related to their radius r, and the lattice spacing d, assuming hexagonal dense packing: $\phi = (16\pi)/3\left(r/(d\sqrt{3})\right)^3$. From the calculated reflection angle, the *apparent* spacings $d_{\rm Bragg}$ and $d_{\rm dyn}$ are found. In Fig. 4b, it is seen that the results of this parameter-free calculation closely track the experimental data for $\Psi = 0.11$. In Fig. 4c ($\Psi = 0.60$), the results are seen to agree with the experiments at longer wavelengths. This confirms that the observed diffraction features of Fig. 3 are caused by close packed layers of colloidal spheres. Thus, this simple model provides a reliable estimate of the crystal spacings in crystals with

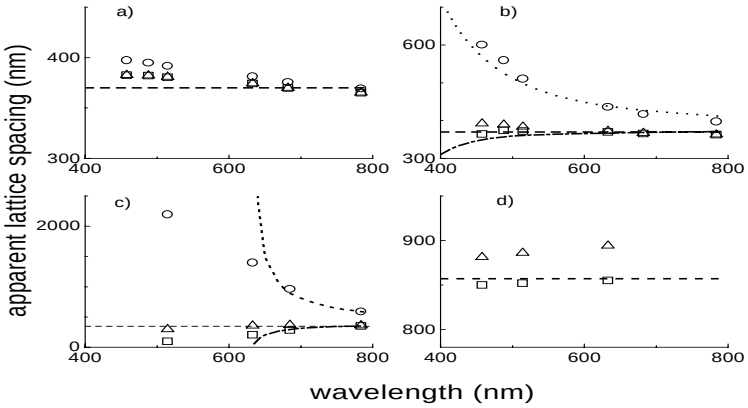

Figure 4. Close packed crystal spacings as a function of the wavelength of light. The long dashed line indicates the expected spacing of the spheres, the circles are Bragg spacings, the squares are spacings calculated with the dynamic theory, and the triangles are Bragg spacings using the average index of the crystal n_{cryst}. The short dashed curves are the Bragg spacings and the dashed-dotted curves the dynamic spacings of the periodically stratified media model. a) spheres with $r = 211$ nm in DMF ($\Psi = 0.017$), b) in H_2O ($\Psi = 0.11$), c) in air ($\Psi = 0.6$), d) spheres with $r = 525$ nm in DMF ($\Psi = 0.017$).

moderate photonic strengths, where the dynamic theory collapses. The deviations at short wavelengths or high energy bands can be explained as follows: in this case, waves are coupled that originate from many different possible hkl reciprocal lattice vectors. The stratified layer model however, only takes into account the vectors with Miller indices $m\,(hkl)$, with m an integer, which clearly gives a worse description for higher bands. Limitations of this model are that the shape of the calculated diffraction pattern differs from the experimental curves, and the width of the diffraction line is strongly overestimated. In fact, the width of the diffraction peak of a single crystal reflects the width of the stopbands. On the other hand however, the width of the diffraction peaks is also influenced by the size of the crystal grains [22], and we believe that in our polycrystalline samples this is the main determining factor.

In the second model, the dielectric constants of the constituent materials are combined to an average n_{cryst} by applying the Maxwell-Garnett theory (see e.g. [32]) to the crystalline configuration of colloidal spheres in the surrounding medium [33]. This produces an average refractive index n_{cryst} that agrees well with the exact solution in the limit $|\mathbf{k}| = 0$ (Fig. 1), but at the same time washes out all crystalline features as well. Therefore, point scatterers are assumed to be present on the positions of the colloidal spheres to account for the diffracted light. The lattice spacings are then calculated with the Bragg law, using n_{cryst} instead of the index of the medium n_{med}. Fig. 4c reveals that this model yields lattice spacings that agree much better with the expected values than both the Bragg or dynamic theories. Indeed Fig. 1 shows that for a dielectric crystal corresponding to Fig. 4c, the diffraction condition is met for 10 % higher energy than in the exact solution. This is in much better agreement with the

exact results than the Bragg result.

In order to probe relatively higher energies in the bandstructures (see Fig. 1), we have also done experiments on close packed crystals ($\phi = 74$ vol%) of much larger spheres ($r = 525$ nm). This corresponds to $d_{\rm hkl}/\lambda$ up to 1.9, compared to 0.8 for the crystals described above. We find that for $\Psi = 0.017$, the dynamic estimate of the lattice spacing is in excellent agreement with the value based on the 2nd and 3rd harmonic of the close packed reflection (Fig. 4d), on independent experiments with confocal microscopy, and on the size of the spheres [34]. The Bragg law combined with the averaged refractive index $n_{\rm cryst}$ gives results that are about 3 % higher. The deviations between these two estimates are contrasted to their excellent agreement in Fig. 4a, and are likely caused by a greater difference between the linear bands using $n_{\rm cryst}$ (effective medium) and the exact bands (Fig. 1). This also indicates that a photonic parameter should include the relevant energy scale. Furthermore, these results illustrate why deviations from the dynamic diffraction theory have not been observed in [15]-[17]: first of all, in those experiments Ψ was less than about 0.05 and secondly, the experiments were done on crystals with much smaller lattice spacings, corresponding to $(d_{\rm hkl}/\lambda) < 0.4$. Finally we note that the parameter Ψ should be improved to take into account excluded volume effects: it has the wrong limit when the volume fraction of high-index material goes to 1, in which case photonic effects are expected to go to zero again. Thus, it seems more reasonable that a photonic parameter scales in such a way that it vanishes in the limit of pure components, $\phi = 0$ or $\phi = 1$. Guidance may be provided by the suggestion of John that photonic band gaps are optimal for $\phi = 1/(2m)$ [11].

6. Conclusions

We have studied colloidal crystals with large refractive index mismatches and strong photonic strengths. We have found that the photonic band structures result in strong dispersion of the apparent Bragg and dynamic lattice spacings. Therefore, diffraction is a useful new method for studying photonic band structures. On the other hand, structural information on the strongly scattering colloidal crystals can be extracted with the aid of simple models. The large index of refraction ratios call for extensions of diffraction theory beyond the well-founded theories known from X-ray diffraction. It is a challenge to calculate the diffraction properties directly from the full band structure.

7. Acknowledgments

We thank Henk Lekkerkerker, Nynke Verhaegh, and David Weitz (Exxon) for useful discussions, and Boris Nieuwenhuis for preparing Fig. 2. This work was part of the research program of the Dutch Organization for Fundamental Research on Matter (FOM) and was made possible by financial support of the 'Nederlandse Organisatie voor Wetenschappelijk Onderzoek' (NWO).

References

1. E. Yablonovitch, Phys. Rev. Lett. **58**, 2058 (1987).
2. S. John, Phys. Rev. Lett. **58**, 2486 (1987).
3. E. Yablonovitch, T. J. Gmitter, and K. M. Leung, Phys.Rev. Lett. **67**, 2295 (1991).
4. "Photonic Band Gaps and Localization," Ed. by C. M. Soukoulis (Plenum, New York, 1993).
5. "Development and Applications of Materials Exhibiting Photonic Band Gaps," Ed. by C. M. Bowden, J. P. Dowling, and H. O. Everitt (J. Opt. Soc. Am. B **10**, 280 (1993)).
6. E. Özbay, E. Michel, G. Tuttle, R. Biswas, K. M. Ho, J. Bostak, and D. M. Bloom, Opt. Lett. **19**, 1155 (1994).
7. See other papers in these Proceedings.
8. M. Born and E. Wolf, "Principles of Optics" (Pergamon, Oxford, 1980).

9. K. M. Ho, C. T. Chan, and C. M. Soukoulis, Phys. Rev. Lett. **65**, 3152 (1990).
10. E. Yablonovitch, see Ref. [4], p. 207.
11. S. John, see Ref. [4], p. 1.
12. R. J. Hunter, "Foundations of Colloid Science," (Clarendon, Oxford, 1992).
13. P. N. Pusey, in "Liquids, Freezing, and the Glass Transition," Ed. by D. Levesque, J.-P. Hansen, and J. Zinn-Justin (Elsevier, Amsterdam, 1990).
14. P. N. Pusey and W. van Megen, Nature (London) **320**, 340 (1986).
15. T. Yoshiyama, I. Sogami, and N. Ise, Phys. Rev. Lett. **53**, 2153 (1984).
16. P. A. Rundquist, P. Photinos, S. Jagannathan, and S. A. Asher, J. Chem. Phys. **91**, 4932 (1989).
17. Y. Monovoukas, G. G. Fuller, and A. P. Gast, J. Chem. Phys. **93**, 8294 (1990).
18. P. L. Flaugh, S. E. O'Donnell, and S. A. Asher, Appl. Spectrosc. **38**, 847 (1984).
19. J. Martorell and N. M. Lawandy, Phys. Rev. Lett. **66**, 887 (1991).
20. C. J. Herbert and M. S. Malcuit, Opt. Lett. **18**, 1783 (1992).
21. W. H. Zachariasen, "Theory of X-ray Diffraction in Crystals," (Wiley, New York, 1945).
22. R. W. James, "The Optical Principles of the Diffraction of X-rays," (Bell, London, 1954).
23. W. L. Vos, R. Sprik, G. H. Wegdam, A. Lagendijk, A. Imhof, and A. van Blaaderen, in "Postdeadline digest, 1994 European Quantum Electronics Conference" (IEEE, Piscataway, 1994).
24. W. L. Vos, R. Sprik, A. Imhof, A. van Blaaderen, A. Lagendijk, and G. H. Wegdam, Phys. Rev. Lett. (submitted).
25. N. Ashcroft and D. Mermin, "Solid State Physics" (Holt, Rinehart, and Winston, New York, 1976).
26. A. van Blaaderen and A. P. M. Kentgens, J. Non-Cryst. Solids **149**, 161 (1992).
27. A. Imhof, A. van Blaaderen, G. Maret, J. Mellema, and J. K. G. Dhont, J. Chem. Phys. **100**, 2170 (1994).
28. A. van Blaaderen and A. Vrij, Langmuir **8**, 2921 (1992).
29. N. A. Clark, A. J. Hurd, and B. J. Ackerson, Nature (London) **281**, 57 (1979).
30. C. A. Murray, W. O. Sprenger, and R. A. Wenk, Phys. Rev. B **42**, 688 (1990).
31. P. N. Pusey, W. van Megen, P. Bartlett, B. J. Ackerson, J. G. Rarity, and S. M. Underwood, Phys. Rev. Lett. **63**, 2753 (1989).
32. See e.g. C. F. Bohren and D. R. Huffman, "Absorption and Scattering of Light by Small Particles," (Wiley, New York, 1983).
33. S. Datta, C. T. Chan, K. M. Ho, and C. M. Soukoulis, Phys. Rev. B **48**, 14936 (1993).
34. A. van Blaaderen and P. Wiltzius, Science, **270**, 1177 (1995).
35. J. B. Pendry, J. Mod. Optics **41**, 209 (1994).